Derivation of guidelines for the design of plate evaporators in heat pumps using zeotropic mixtures

Elmegaard, Brian; Mancini, Roberta; Zühlsdorf, Benjamin

Published in:
Proceedings of ECOS 2017: 30th International Conference on Efficiency, Cost, Optimization, Simulation and Environmental Impact of Energy Systems

Publication date:
2017

Document Version
Peer reviewed version

Derivation of guidelines for the design of plate evaporators in heat pumps using zeotropic mixtures

Roberta Mancini[a], Benjamin Zühlsdorf[b] and Brian Elmegaard[c]

[a] Technical University of Denmark, Kgs. Lyngby, Denmark, robman@mek.dtu.dk
[b] Technical University of Denmark, Kgs. Lyngby, Denmark, bezuhls@mek.dtu.dk
[c] Technical University of Denmark, Kgs. Lyngby, Denmark, be@mek.dtu.dk

Abstract:

The present work derives design recommendations for plate heat exchangers used for evaporation of zeotropic mixtures in heat pumps. A parametric study is conducted on the geometry of the heat exchanger, and the analysis is carried out for four working fluids, based on a case study of heat pump integration in a spray drying facility. A numerical model of the evaporator is combined with cycle calculations, for estimating the impact of heat transfer area and pressure drop on the coefficient of performance and costs. Common trends are obtained as optimal configurations for the four considered fluids. It is recommended to minimize the hydraulic diameter by employing high corrugation height over low corrugation pitch. Moreover, an optimal range is found for the liquid Reynolds number at the evaporator inlet. The suggested values vary between 500 and 2000, depending on the fluid. Lastly, the trade-off between minimization of area and pressure drop is found by assessing the relative impact on costs of the heat exchanger area and pressure losses of both working fluid and heat source. The result shows that it is not always convenient to minimize the heat transfer area, since the mixture pressure drop negatively influences compressor investment and operating costs.

Keywords:

Plate heat exchangers, Waste heat recovery, Zeotropic mixtures, Heat pumps, Cost optimization.

1. Introduction

Implementation of energy efficiency measures in the industry sector is becoming imperative due to the increasing awareness of the environmental effects of fossil fuel consumption. The total energy consumption of the Danish industry sector accounted for 112 PJ in 2012. Drying processes alone constituted 19% of the consumption. Moreover, drying processes are a relevant source of waste heat, specifically around 7% of the total industrial waste heat [1]. Waste heat recovery is accordingly one suitable opportunity for increasing energy efficiency of drying processes. One possibility of recovering low grade thermal energy is the integration of heat pumps, which are able to lift the temperature level of the waste heat, in order to meet the energy needs of many industrial sectors [2].

Zeotropic mixtures constitute one possibility of optimizing the heat pump coefficient of performance (COP) by reducing the irreversibility in the heat exchangers. In fact, the exergy destruction in the evaporator and condenser due to finite temperature difference between the working fluid and the heat source or sink can be reduced by matching the mixture temperature glide with the heat source or heat sink temperature profiles [3].

However, the use of zeotropic mixtures implies a degradation of the heat transfer coefficient during both evaporation and condensation. During flow boiling in the heat exchanger channels, an additional mass diffusion resistance is created because of the more readily evaporation of the more volatile component. This phenomenon correspondingly entails an increase of the saturation temperature of the mixture, which becomes richer in the less volatile component. Moreover, a decrease of the nucleate boiling contribution is estimated, together with a degradation of the mixture transport properties with respect to pure components. Altogether, the aforementioned mechanisms lead to

worse heat transfer for zeotropic mixtures compared to pure fluids [4]. For this reason, when optimizing cycle performances by means of zeotropic working fluid mixtures, it is of high relevance to optimize the design of the heat transfer equipment, in order to avoid investing in higher heat transfer areas for the heat exchangers.

Plate Heat Exchangers (PHEs) offer a suitable solution for applications with zeotropic working fluid mixtures, since it is possible to achieve high heat transfer coefficients due to the flow turbulence generated by the characteristic plate corrugation patterns. Chevron-type plates are commonly employed to create such corrugations. Moreover, PHEs offer a modular and flexible solution, i.e. variation of thermal capacity can be simply obtained by changing the number of plates in the frame. Plate heat exchangers consist of thin parallel plates stacked together in order to form channels for fluid flow. Gasketed-type PHE consist of plates sealed by gaskets and held together by a frame. For higher operating temperature and pressure, the plates can be sealed together by brazing. The flow can be arranged in counter-current, thus making them a viable option to achieve the glide matching between zeotropic mixture and heat source or sink. At current state-of-the-art, the operability limits of gasketed-type PHEs is limited to 20.4 bar and 150°C as maximum pressure and temperature, respectively, hence offering a reasonable range for operation as evaporators in heat pumps [5].

Scientific literature provides a number of studies focusing on PHE design optimization for low temperature applications, most of them for organic Rankine cycles (ORCs). Gut and Pinto (2004) [6] developed an optimization program to determine the optimal configuration of PHEs for a given imposed maximum pressure drop and inlet fluid flow velocity; the optimization was based on the minimization of the heat transfer area. The work did not take an optimal choice of the pressure and velocity limitations for different applications into account, and did not consider the impact of the PHE on the thermodynamic cycle. Karellas et al. (2012) [7] investigated the influence of supercritical ORC parameters on PHE design. The study fixed the corrugation geometry and hydraulic diameter of the evaporator for the analysis, and assessed the difference of required heat transfer area for different fluids and cycle parameters, yet without considering pressure drops. Wang et al. (2013) [8] performed a multi-objective optimization procedure with the aim of minimizing heat transfer area and pressure losses of a PHE condenser in an ORC. The results showed the sensitivity of three design parameters of the PHE, namely plate length, width and corrugation height, on the heat exchanger area and pressure drop. Rohmah et al. (2014) [9] investigated the influence of plate spacing on condenser design for a ORC. It was shown that increasing the plate spacing led to an increase of the required area but a decrease of related pressure drop. Walraven et al. (2014) [10] developed a combined optimization procedure of a low temperature heat source ORC and heat exchangers, considering both PHE and shell and tube configurations. The optimization was aimed at maximizing the cycle exergy efficiency by changing both cycle and heat exchanger design parameters. The results showed that optimal PHE configurations performed better than shell and tube for most working fluids.

The main objective of the present work is to derive design recommendations for PHEs used as evaporator in heat pumps using zeotropic mixtures. The methodology is based on assessing the impact of the PHE design parameters on the cycle COP and Net Present Value (NPV). The analysis is based on four different working fluid mixtures, found as the best solutions for heat pump integration in a spray drying facility in [3]. The study focuses on the evaporator section of the PHE because the evaporator outlet condition is directly affecting the compressor work in the cycle. In order to carry out the analysis, a design model is developed to assess the required heat transfer area and resulting pressure losses for the working fluid and the heat source. The heat exchanger design model is coupled with heat pump calculations and the pressure drops are taken into account for the estimation of the COP and NPV of the cycle. The results are analysed in order to derive more general design guidelines for the evaporator section, which can be used in similar applications.

The framework of the analysis is given by a previously conducted study [3], assessing the integration of high temperature heat pumps in a spray drying facility, exploiting excess heat at 65°C for pre-heating of air up to 120°C. The advantage of using zeotropic mixtures was demonstrated by comparing the COP and NPV of a simple configuration of a vapor compression heat pump, in which

the working fluid was varied based on binary mixtures formed by combinations of six different hydrocarbons. It was shown that the best fluids corresponded to the ones better matching the heat sink and source temperature profiles, and a group of optimal mixtures was found. The sizing of the PHEs for economic calculations was based on a minimum pinch point temperature difference and maximum allowable velocities for liquid and gas phases, based on limiting values found in literature [11], and posing a constraint on the free flow area of the fluids in both evaporator and condenser. This criterion is based on empirical experience from manufacturers and the extension to other type of applications (e.g. phase change and/or zeotropic mixtures) is not trivial. Therefore, the derivation of specific design criteria for PHE design in such applications is the research question behind this work.

2. Methods

In order to derive design guidelines, a parametric study was conducted on the geometry of the PHE, used in the evaporator. For the assessment of the impact of the heat exchanger design on the cycle COP and NPV, a detailed numerical model of the heat exchanger was built and integrated with the previously presented heat pump model [3] in the Matlab [12] simulation environment. The working fluid properties were calculated by means of the database Refprop [13], using standard equation of states and mixing parameters.

Four different analyses were done to highlight common design trends of geometrical and fluid flow parameters, based on the four best working fluids found from the previous study [3]. Table 1 presents the evaporation pressure of the four cases, well below the maximum operability limit, showing that PHEs constitute a feasible design for all the cases. The working fluids are given by the four hydrocarbon mixtures reported in Table 1 with relative compositions. The heat pump was designed for waste heat recovery of air, with an available mass flow rate of 14.8 kg/s and inlet and outlet temperatures of 65°C and 40°C, resulting in a heat source capacity of 1544 kW. A minimum pinch temperature difference of 10°C was imposed over the heat exchanger. For all the cases, a minimum super-heating of 5°C before the compressor is included in the evaporator.

Table 1. Summary of the four cases considered in the analysis, with required evaporation pressure and results obtained from the study [3]

Case	Working fluid	p_{ev}, bar	$\dot{V}_{comp_{in}}$, m^3/h	COP, -	NPV, € 10^3
I	Propane – Iso-Pentane (0.5/0.5)	4.9	2220	3.08	921
II	Propane – n-Pentane (0.8/0.2)	8.4	1487	3.04	998
III	Propane – n-Pentane (0.4/0.6)	3.0	3288	3.02	419
IV	Butane – Hexane (0.9/0.1)	2.5	3668	3.07	509

2.1. Plate Heat Exchanger parametric analysis

The geometrical parameters of PHEs were given by the plate size, namely width W and length L_{th}, the number of channels N_{ch} and the corrugation characteristics, i.e. the corrugation height b, the corrugation pitch Λ, the chevron angle β and the plate thickness t. The plate thickness t was fixed to a constant value usually found in common PHE design, minimizing the conductive heat transfer resistance and providing acceptable mechanical strength. The port diameter size D_p was chosen between two values, depending on the plate size W. Fig. 1 shows the plate geometry and corrugations. The corrugation parameters determine the hydraulic diameter of the PHE channels, hence defining the fluid conditions during the flow inside the channels. The hydraulic diameter was estimated by (1), describing the relation between corrugation height b and enlargement factor Φ. The latter represents the ratio between the actual area of the corrugated plate and the projected flat plate area, and it is expressed by (2) as function of the corrugation pitch and height [14].

$$D_h = \frac{2b}{\Phi} \tag{1}$$

$$\Phi = \frac{1}{6}\left(1 + \sqrt{1 + \left(\frac{\pi b}{\Lambda}\right)^2} + \sqrt{1 + \frac{1}{2}\left(\frac{\pi b}{\Lambda}\right)^2}\right) \quad (2)$$

The design parameters were varied among the values reported in Table 2, investigating all possible combinations. The plate length, shown as L_{th} in Fig. 1, was calculated from the input geometry by means of the design model in order to match the heat transfer demand.

Table 2. Geometrical parameters of the PHE, with values considered in the parametric analysis

Parameter	Unit	Values
W	m	0.1 – 0.3 – 0.5 – 0.7 – 0.9
N_{ch}	-	10 – 20 – 40 – 70 – 100
β	°	20 – 45 – 60 – 80
b	mm	2 – 5 – 8
Λ	mm	2 – 5 – 8
t	mm	0.5
D_p	m	0.05 – 0.15

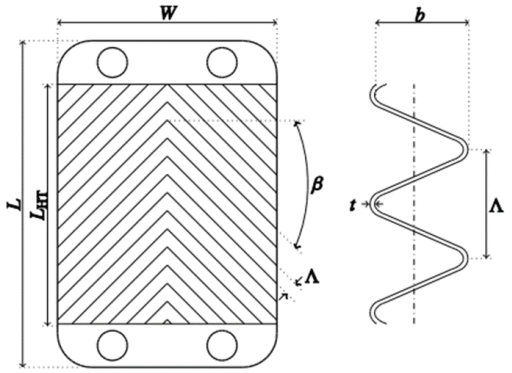

Fig. 1. Schematic view of a chevron-type PHE [15]

2.2. Mathematical model

In this section, the different parts of the numerical design model are presented and discussed, i.e. the heat transfer and fluid flow model describing the heat exchanger and the integration with the heat pump model, including economic calculations of the cycle.

2.2.1. Plate heat exchanger numerical model

The numerical model of the PHE was based on a one-dimensional discretization along the flow direction. The discretization took into consideration equidistant steps of enthalpy rate change for both the fluids. The heat transfer and fluid flow conditions were solved for each control volume (CV), hence heat transfer area and pressure drops were calculated for each element. The temperatures for heat transfer calculations were estimated at the CV centre points, interpolating the values between the nodes. Pressures and enthalpies were calculated at the nodes. The input to the PHE model were given by the cycle calculations, i.e. known inlet mass flow and thermodynamics for the two fluids, as well as outlet enthalpies. The model calculated the outlet temperature and pressure levels.

The heat transfer was solved by calculating the overall heat transfer coefficient in each CV [14], expressed by (3), with R^i_{wall} representing the specific conductive resistance of the plate wall, and h^i_{mix} and h^i_w representing the heat transfer coefficients of the mixture and water for the *i*-th CV.

$$U^i = \left(\frac{1}{h^i_{mix}} + R^i_{wall} + \frac{1}{h^i_w}\right)^{-1} \quad (3)$$

The heat transfer coefficients were calculated for each control volume, since they were dependent on the fluid properties, temperature and specific heat flux. The water side heat transfer coefficient was modelled by using the correlation of Martin (1996) [16], which is valid for PHEs with chevron-type corrugations and allows the estimation of the friction factor and Nusselt number for single-phase flow. The mixture heat transfer coefficient was estimated according to the CV location in the PHE; more specifically, if the fluid was in the evaporator section, a specific correlation developed for zeotropic mixtures was employed in order to consider the mixture effects on heat transfer. The correlation of Jung (1989) [17] was chosen for the analysis, based on a superposition model with two contributions from convective and nucleate boiling, and correction parameters taking into

consideration the deviation from ideal mixing. The super-heating section was modelled by considering the same correlation used for water, being the working fluid in the single-phase region.

The fluid flow was modelled by calculating the pressure level at each node of the CVs. The pressure drop along the channel derives from both friction and acceleration contributions. The pressure drop of the water flow and of the mixture flow in the super-heating section were calculated by considering the contributions of friction and acceleration, by using (4) [14], where the friction factor f derives from Martin (1996) [16]. The losses are expressed as function of the length of the CV, the fluid properties, mass velocity G and equivalent diameter D_e, equal to $2b$.

$$\Delta p_{\text{core}} = \Delta p_{\text{fr}} + \Delta p_{\text{acc}} = 4f\Delta L \frac{G^2}{2D_e}\left(\frac{1}{\rho}\right)_m + \left(\frac{1}{\rho_o} - \frac{1}{\rho_i}\right) G^2 \tag{4}$$

The frictional and acceleration pressure losses for the two-phase region of the zeotropic mixture were calculated by means of the Jung and Radermacher (1989) [18] correlation for the frictional contribution, while the Martinelli and Nelson (1984) [4] two-phase slip flow model was adopted to account for the acceleration term. In addition to the core pressure drop, another term was added to the heat source pressure drop: the port pressure drop of the PHE inlet was considered, since it has an impact on the overall pumping costs for the water side. On the other hand, it was decided to neglect the port pressure drop of the evaporator inlet for the mixture, since the throttling valve will implicitly balance the effect. The port pressure drop was calculated as reported in Shah (2002) [14].

The sizing procedure can be outlined as follow. First, the thermodynamics at each node of the heat exchanger was determined by assuming constant pressure over the length. The energy balance in each CV allowed the calculation of the UA value. The discretized area required for the heat transfer in each control volume was estimated by calculating the overall heat transfer coefficient *U*, as shown in (3). Once that the required length was determined from the area, the pressure drop of both fluids was determined and to the values of temperature and pressure at each node of the heat exchanger were found. The procedure of the PHE model is summarized in Fig. 2 (a). The convergence criterion was defined by a tolerance fixed to 10^{-4}. For the parametric analysis, a number of 20 control volumes and 21 nodes was used, chosen as a trade-off between computational cost and accuracy.

2.2.1.1. Analysis of flow parameters

When considering flow boiling of zeotropic mixtures, several parameters can be taken into account for a full description of the flow mechanism. Both vapour and liquid phases flow inside a channel, and the vapour and liquid mass flows and velocities strongly depend on the stage of the evaporation process. Moreover, the liquid and vapour phase compositions are not constant during evaporation of mixtures, because of the more volatile component evaporating first, hence a strong variation of the mixture properties was experienced during the process [4]. Despite the complexity of the physics, there is the need to choose a meaningful design parameter, which encapsulates information on the fluid, and on the conditions of the flow at some relevant positon along the PHE. Therefore, it was decided to analyse the influence of the Reynolds number of the liquid phase at the inlet of the evaporator. The parameter is defined by (5) [4], as function of the mass velocity G, vapor quality Q, channel hydraylic diameter D_h and viscosity of the liquid phase μ_L.

$$\text{Re}_L = \frac{G\,(1-Q)\,D_h}{\mu_L} \tag{5}$$

The mass velocity G was given by (6) [14], as function of the mass flow of the mixture and of the PHE geometrical parameters determining the free flow area , namely corrugation height b, plate width W and number of channels N_{ch}.

$$G = \frac{\dot{m}_{\text{mix}}}{bWN_{\text{ch}}} \tag{6}$$

The mass flux contains information on the fluid, as well as on the geometry of the PHE, i.e. hydraulic diameter, corrugation height, width and number of channels are considered for the calculation. Moreover Re_L was used for the estimation of the heat transfer coefficient in the correlations for flow boiling of zeotropic mixtures, hence its value was directly affecting the sizing of the PHE. Additionally, it was decided to analyse the behaviour of the Reynolds number at the location of evaporator inlet, because the inlet temperature and pressure are less affected by the pressure losses compared to the evaporator outlet. In fact, the inlet quality and viscosity were dependent only on the cycle configuration (state point at the evaporator inlet), and the design of the heat exchanger directly influenced the flow conditions at this position.

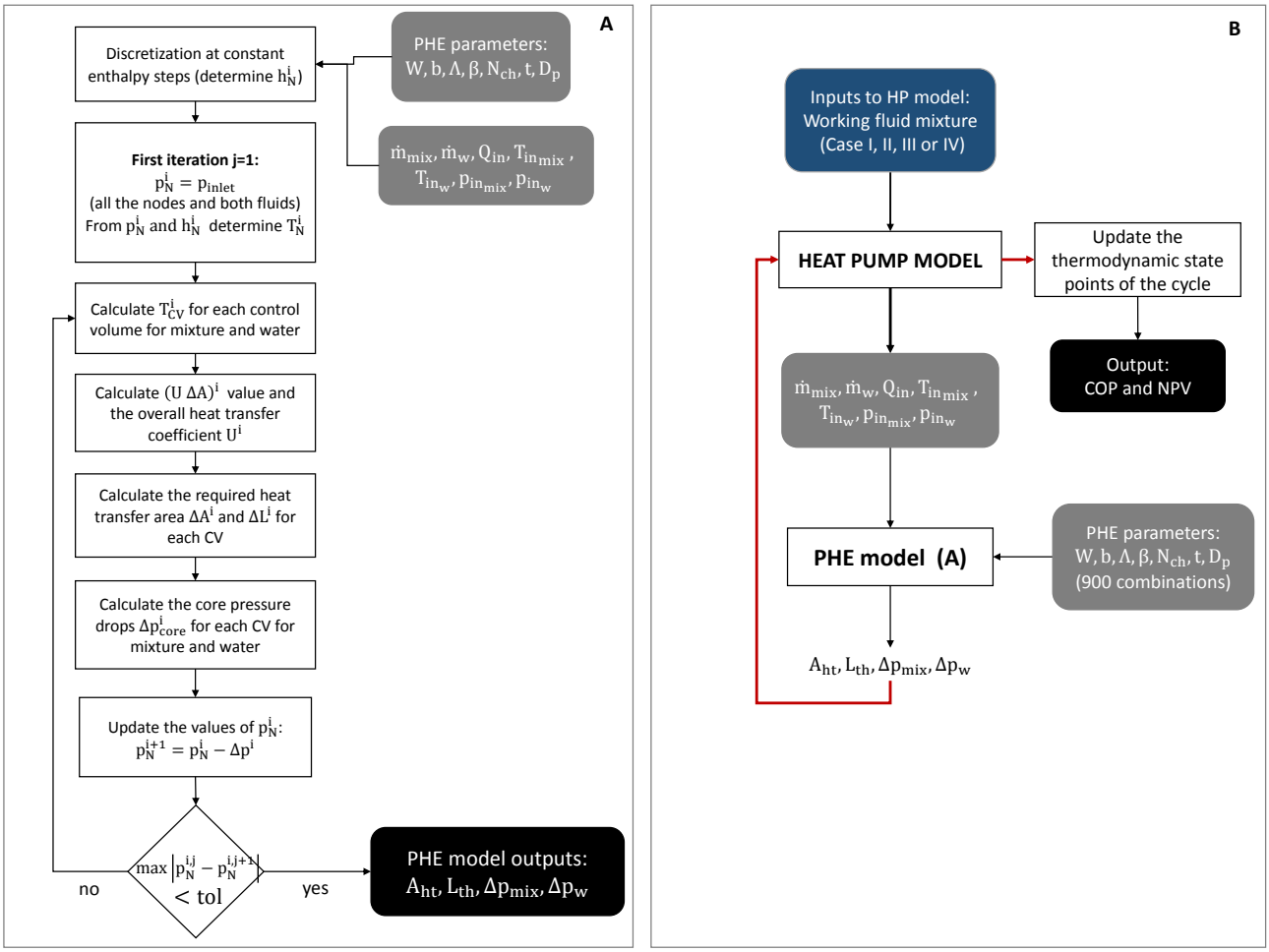

(a) (b)

Fig. 2. a) Procedure for PHE sizing and b) integration with the heat pump and overall methodology

2.2.2. Heat pump model and economic calculations

Fig. 2 (b) reports the procedure of the integration of the heat pump model with the PHE model. The procedure was carried for all the combinations of PHE design parameters and the four different working fluid mixtures. The heat pump was first solved for the calculation of the inlet and outlet states at the evaporator. Next, the PHE model solved the heat transfer and fluid flow equation, while determining the heat transfer area. This procedure was repeated for all the combinations of design parameters, each giving different required heat transfer areas and different outlet pressure and temperature (corrected by the pressure drop). The heat pump model received the output of the PHE model, and calculated the COP and the NPV again, by taking into account the updated temperature and pressure at the evaporator outlet. The COP was affected by the change in compressor power as function of the mixture pressure drop. On the other hand, different aspects of the PHE design

influenced the value of the NPV of the heat pump. The NPV was calculated by (7) [3], as function of the Total Capital Cost (TCI), Operation and Maintenance Cost (OMC), the Fuel Cost (FC_{hp}) due to the compressor, the required water pumping cost (FC_w), as well as the natural gas saving FC_{ng}.

$$NPV = -TCI - OMC - \frac{FC_{hp}}{CRF} - \frac{FC_w}{CRF} + \frac{FC_{ng}}{CRF} \tag{7}$$

OMC and F_{ng} are calculated as explained in [3], while the other contributions are adjusted according to the PHE model outputs. TCI accounts for the investment of condenser, compressor and evaporator. The latter was estimated using the sizing of the heat transfer area from the PHE model, while the condenser heat transfer area was fixed according to the design criterion applied in [3]. The TCI of each component was calculated from the Purchased Equipment Cost (PEC), scaled according to the component size with scaling factors reported by [19]. The TCI was increased by a factor 4.16 compared to the PEC, to account for the investment of the expansion of an existing facility, as reported in [19]. Since the compressor power was adjusted according to the PHE design, the investment cost varies accordingly. The running cost of the compressor, given by FC_{hp}, was adapted to the updated compressor power. The addition of the fuel cost term for the pressure losses of the heat source (water) side, is calculated by using (8), as function of the water mass flow rate $\dot{m}_w$, water density ρ_w, total water pressure drops $\Delta p_{w_{tot}}$,a pump efficiency η_{pump} equal to 95%, the electricity cost c_{el} assumed equal to 0.0783 €/kWh and annual operation hours τ_h equal to 7400 h/y.

$$FC_w = \frac{\dot{m}_w}{\rho_w}\frac{\Delta p_{w_{tot}}}{\eta_{pump}} c_{el}\tau_h \tag{8}$$

The interest and inflation rates were assumed equal to 7% and 2%, respectively, and then used for the estimation of the Capital Recovery Factor (CRF), with a plant economic lifetime of 20 years [19] [20]. The annual Operation and Maintenance Cost (OMC) were analogously to [3] calculated as a one-time fixed share of the initial investment cost of 20 % at the investment time, and the saving of natural gas consumption (F_{ng}) was calculated by considering a boiler efficiency of 90 % [19] [20] . The reader is referred to [3] for more details on how the heat pump model is built. Fig. 3 (a) shows the flow sheet of the heat pump model, with evaporator and condenser, and the processes occurring in the components. Fig. 3 (b) shows the log(p)-h diagram of the heat pump with and without pressure drops in the evaporator. It can be noticed how the outlet of the evaporator is affected by the pressure losses, thus changing the compressor power required. The pressure drop influences also the evaporator inlet location in the diagram, but to a lower extent compared to the outlet.

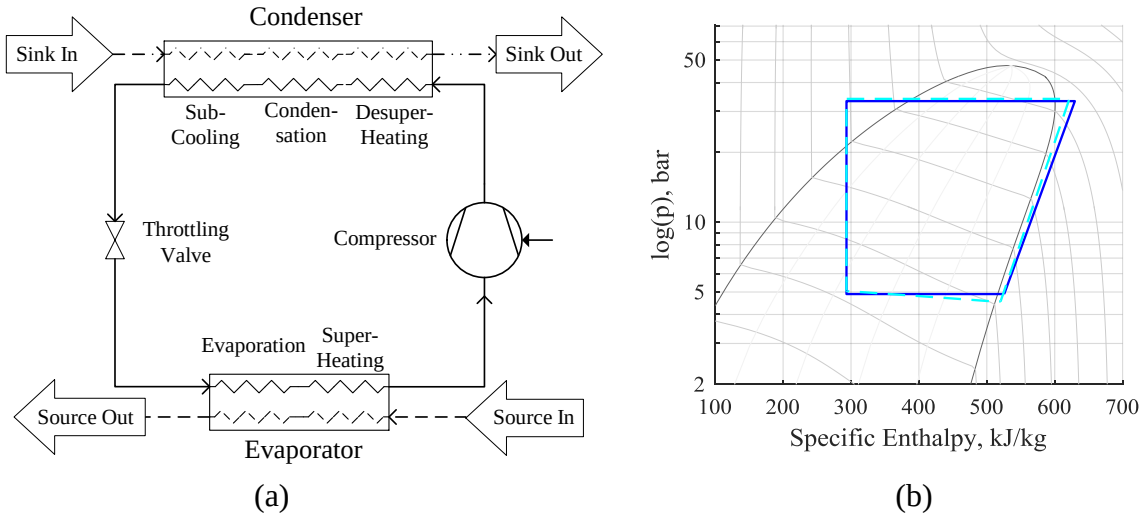

Fig. 3. (a) Flow sheet of the heat pump model and (b) log(p)-h diagram of the thermodynamic cycle without pressure drop (blue) and with 50 kPa pressure drop in the evaporator (light blue)

3. Results

3.1. Heat transfer area and pressure drop trade-off

Fig. 4 shows the NPV of the heat pump as function of the heat transfer area of the evaporator, for all the combinations of design parameters and for all the four zeotropic mixtures. Each point in the figure corresponds to one possible combination of the different design parameters. The colour scale represents the total pressure drop of the working fluid mixture. First, all the four cases considered reported similar trends on how the area and the pressure losses affect the performance of the system. By having high heat transfer area, the NPV decreased consistently because of the higher investment costs of the PHE. On the other hand, high pressure losses negatively affected the NPV even for those configurations with minimal PHE area.

This result highlights the importance of including the impact of pressure losses when assessing the profitability of the heat pump, since the impact on the NPV was relevant for all the cases. The optimal

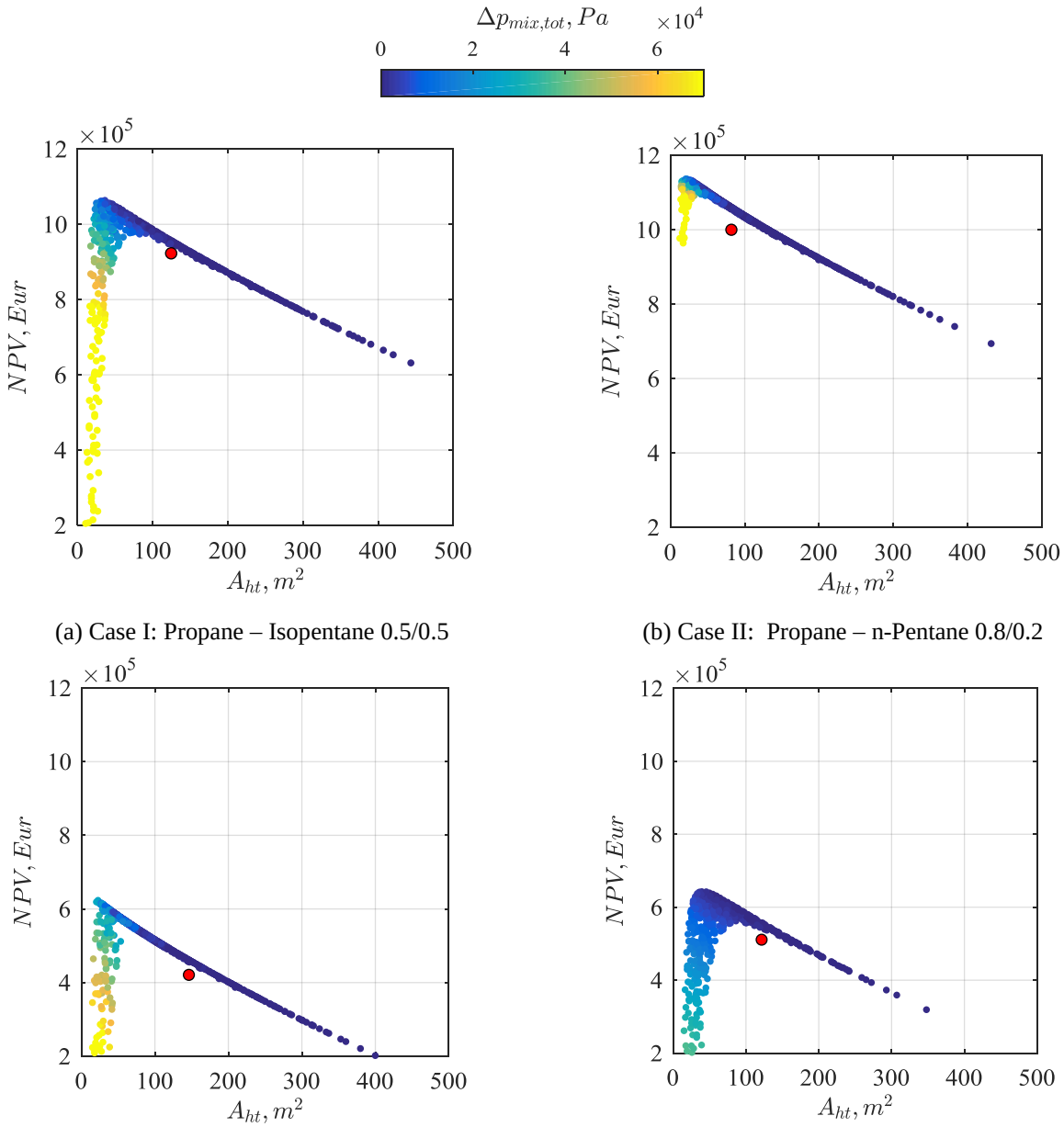

(a) Case I: Propane – Isopentane 0.5/0.5

(b) Case II: Propane – n-Pentane 0.8/0.2

(c) Case III: Propane – n-Pentane 0.4/0.6

(d) Case IV: n-Butane – n-Hexane 0.9/0.1

Fig. 4. NPV vs. PHE area, for Case I (a), Case II(b), Case III(c) and Case IV(d), with colour indicating the mixture pressure drop and red point showing the design criterion adopted in [3].

regions corresponded to combinations of design criteria giving small heat transfer area (hence low investment cost) together with reasonable pressure losses of the working fluid mixture. Values of pressure losses between 5 kPa and 30 kPa were optimal for all the four cases, as shown by the colour of the design points where NPV is maximal. Moreover, the red points in Fig. 4 indicate the design criterion adopted in the previous analysis of the case study [3]. As aforementioned, the design was based on posing a limitation on the inlet velocities of cold and hot fluids, not specifically derived for evaporation of zeotropic mixtures. It is shown that the economic optima did not coincide with the old design criterion, since a better NPV can be obtained by changing the design parameters in all the cases. The red point does not lie in the same design curve of the present analysis, since the reduction of required heat transfer area due to the pressure drop was not considered in the previous study [3].

The relative ranking of the four working fluid mixtures with respect to NPV was unchanged compared to the previous results [3], with Case I and Case II showing results with a more advantageous economy, i.e. NPV around the double for the optimal regions in both cases. Therefore, the PHE design does not affect the choice of the optimal mixture for this specific case study of heat pump integration. The following step of the results analysis consists in the identification of design and flow parameters describing the PHE in the optimal region. In order to do this, the relation between heat transfer area and NPV is presented as function of the main design parameters, so that the identified optimal region can be related to optimal values of the geometry and flow parameters of the heat exchanger.

3.2. Influence of the corrugation geometry

The corrugation height b, the corrugation pitch Λ and the chevron angle β are the geometrical parameters of the chevron-type PHE defining the type of corrugation used, influencing the flow condition inside the channels. The corrugation pitch and height define both the hydraulic diameter, used for heat transfer and pressure drop correlations, and a characteristic corrugation parameter X, defined as $b\pi/\Lambda$. The corrugation parameter X is directly related to the estimation of Φ, i.e. the ratio of the actual area over the projected flat area, introduced by (2). Fig. 5 represents the NPV and the heat transfer area A_{ht} for Case I. In Fig. 5(a) the colours indicate the hydraulic diameter of the channels, while in Fig. 5(b) the corrugation characteristic X is shown. It can be seen that it was optimal to employ corrugations leading to low hydraulic diameters, since a higher degree of turbulence was reached and heat transfer was enhanced. However, the best configurations were the ones for which the corrugation parameter X was very high. This means that it was preferred to achieve such small hydraulic diameter by manufacturing corrugation with high values of the corrugation height b and low values of the corrugation pitch Λ. From the analysis, it was shown that such configurations were the ones enhancing heat transfer without impacting negatively on the pressure losses. Therefore, it was concluded that all the optimal points in the figure were the ones corresponding to X above 10,

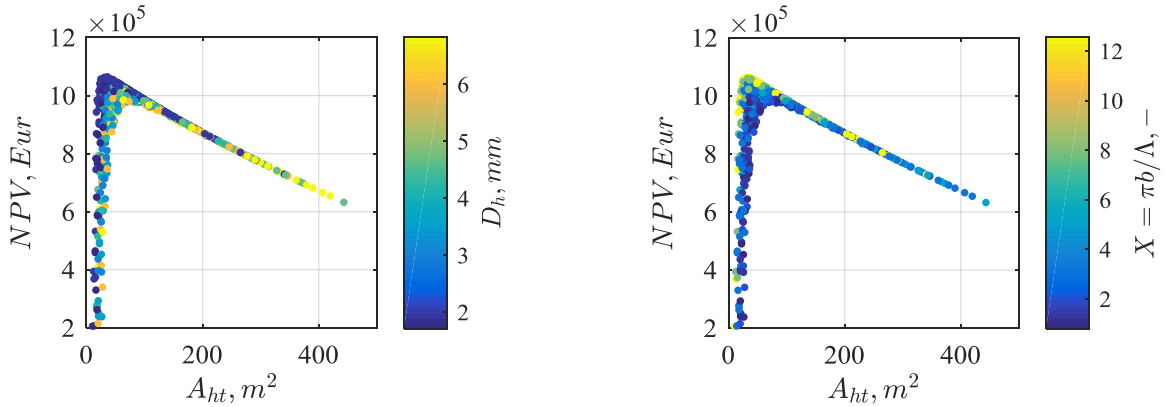

Fig. 5. NPV as function of the heat transfer area, with colour indicating the magnitude of the hydraulic diameter (a) and the corrugation characteristic X (b). The results refer to Case I.

hence with b close to the value of 8 mm and Λ to the minimum value set as 2 mm. Analogous trends were observed for Cases II, III and IV, validating the conclusion, so they are not reported as figures.

Another parameter directly affecting the corrugation of the PHE, was the chevron angle β, with results shown in Fig. 6 (a) for Case I and Fig. 6 (b) for Case II. An analogous behaviour was observed for the two cases. There was not a clear trend as the one observed for the previous parameters, however it was shown that it was preferable to adopt angles in the higher range (above 60°), and that solutions around this median value seemed to be more optimal compared to the ones with very high angle (80°). Therefore, for this application, chevron angles within the range of 40° to 60° should lead to economically advantageous PHE design.

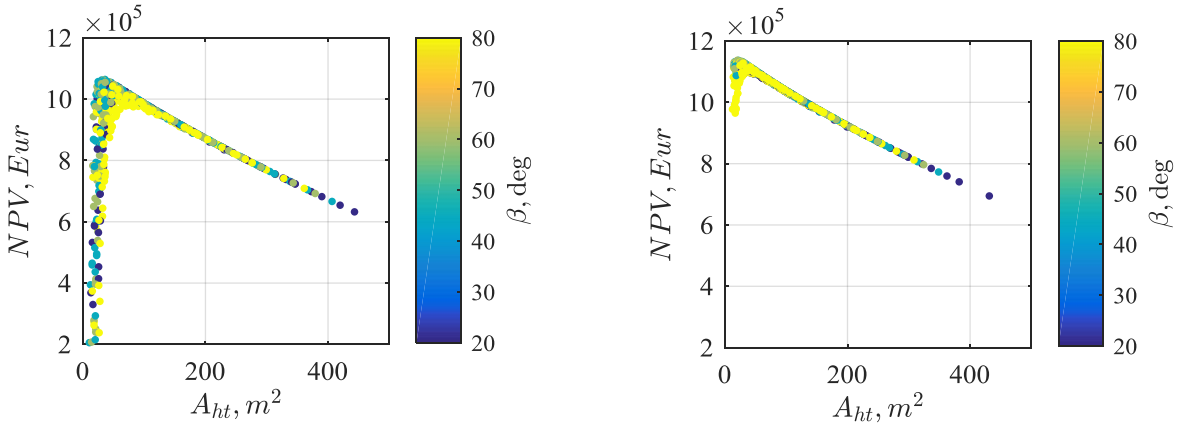

Fig. 6. NPV as function of the heat transfer area, with colour indicating the chevron angle for Case I (a) and Case II (b).

3.3. Influence of the plate size and numbers

Other geometrical parameters affecting the design of PHEs were the plate size and number of plates forming the flow channels. The results are reported in Fig. 7 (a), for Case I and Fig. 7 (b) for Case II.

The abscissa axis reports the values of the length-to-width ratio while the colour indicates the number of channels employed. It must be mentioned that configurations with length-to-width ratios below unity are not commonly found in the current market of PHEs, but usually ratio above 1 are adopted by manufacturers [21] [22]. However, it was decided not to limit the analysis to fixed values of the length-to-width ratio, in order to show the complete range of optimal solutions calculated by the PHE numerical model.

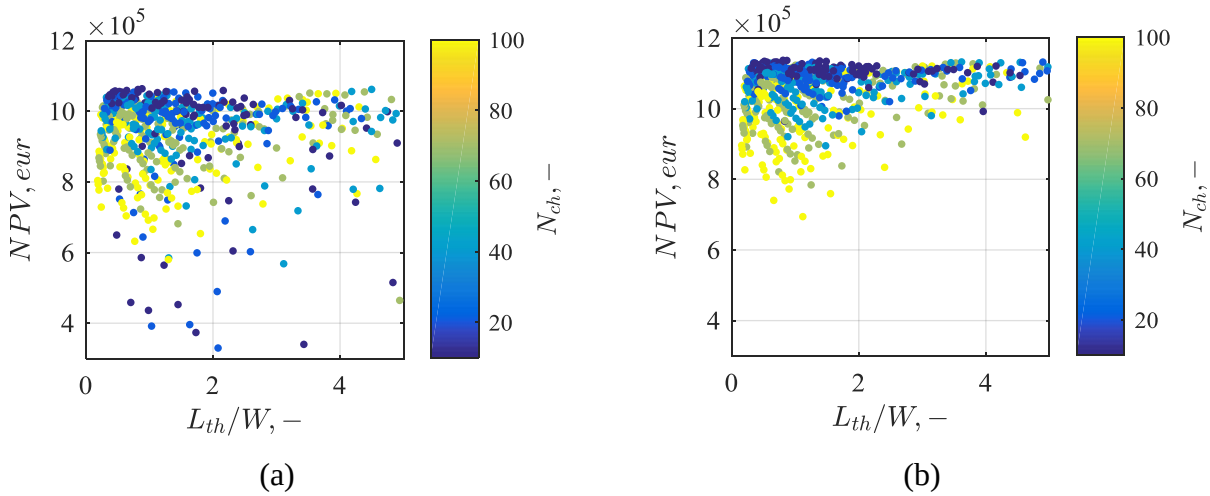

Fig. 7. NPV vs L/W , with colour indicating number of channels for Case I (a) and Case II (b)

From the results, it is shown that the highest values of NPV were reached by configurations with very different values of the ratio, and adjusting the number of channels used. Specifically, by employing plates with lower values of length-to-width ratio, a lower number of channels was required and preferred for optimal solutions, while the opposite trend is observed for higher values of ratio. Therefore, when designing a PHE, the plate size and number can be decided by considering other constraints, e.g. commercial availability or ease of manufacture, and the geometry of the corrugation might constitute the main parameters left as design variables. The plate size did not affect the results consistently, i.e. optimal configurations can be built by using different combinations of plate size and number of channels.

3.4. Flow parameters

Another analysis aimed at showing the relation between the flow conditions of the working fluid mixture inside the channels of the PHEs and the NPV of the cycle. The results are shown in Fig. 8, for the four cases considered, and it was observed that analogous trends were obtained with the optimal NPV lying in the same region of Reynolds numbers.

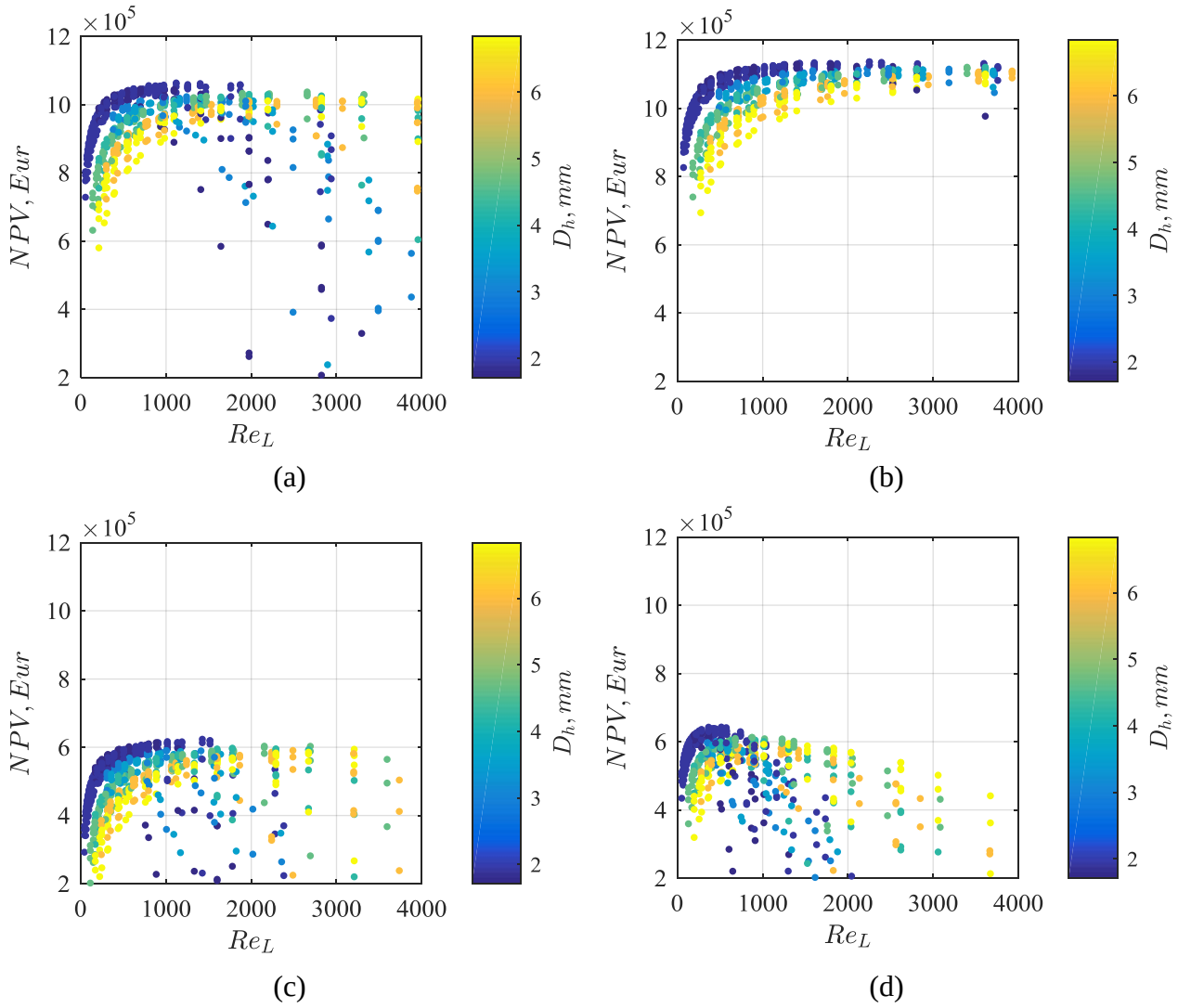

Fig. 8. Reynolds number of the liquid phase vs. NPV at the evaporator inlet for Case I (a), Case II (b), Case III (c) and Case IV (d), with colour indicating the value of hydraulic diameter.

The NPV is reported as function of Re_L. The point colour indicates the hydraulic diameter employed to achieve the flow condition. It can be seen that the highest curves for NPV are all obtained by choosing configurations with the minimum hydraulic diameters. Furthermore, it can be seen that the optimal range for Re_L lies within a range of 500-2,000, depending on the case considered. Case I and

III presented the peak of the NPV with a Reynolds number close to 1,000-1,500, while Case II showed a flatter trend of the NPV, with the highest points achieved around the value of 2,000. Case IV presented the maximum with lower Reynolds numbers between 500 and 1,000. The difference was related to the different properties of the working fluid mixtures. However, it was observed that the trends were analogous in all the cases, and the optimal range was within the specific region of 500-2,000, which could be therefore considered as a recommended range for the flow of the liquid phase at the evaporator inlet. Lastly, it is worth it to mention that a value of 1,000 for the Reynolds number for Case I corresponded to a liquid velocity of 5 m/s. The design criterion used in the previous analysis [3] was a limit velocity of 2 m/s. The results confirmed how the best NPV deviates from this value.

3.5. Cost analysis

As aforementioned in 2.2.2, the NPV was affected by the design parameters according to different contributions. The impact of the design on the various terms contributing to the NPV is shown for Case I. The PHE design was expressed by the heat transfer area A_{ht}, while the NPV value was divided into a term indicating the revenue (natural gas saving), and a term indicating the total cost, as shown in Fig. 9 (a) and (b). The former shows the variation of the cost for the total solution space, constituted by PHE with A_{ht} ranging from around 10 m^2 up to around 500 m^2; the latter shows a close-up of (a), where only solutions with area up to 50 m^2 are reported, so that the trends are better highlighted.

In the figure, the cost contribution is divided into the different terms, adjusted by the CRF as indicated by equation (5).

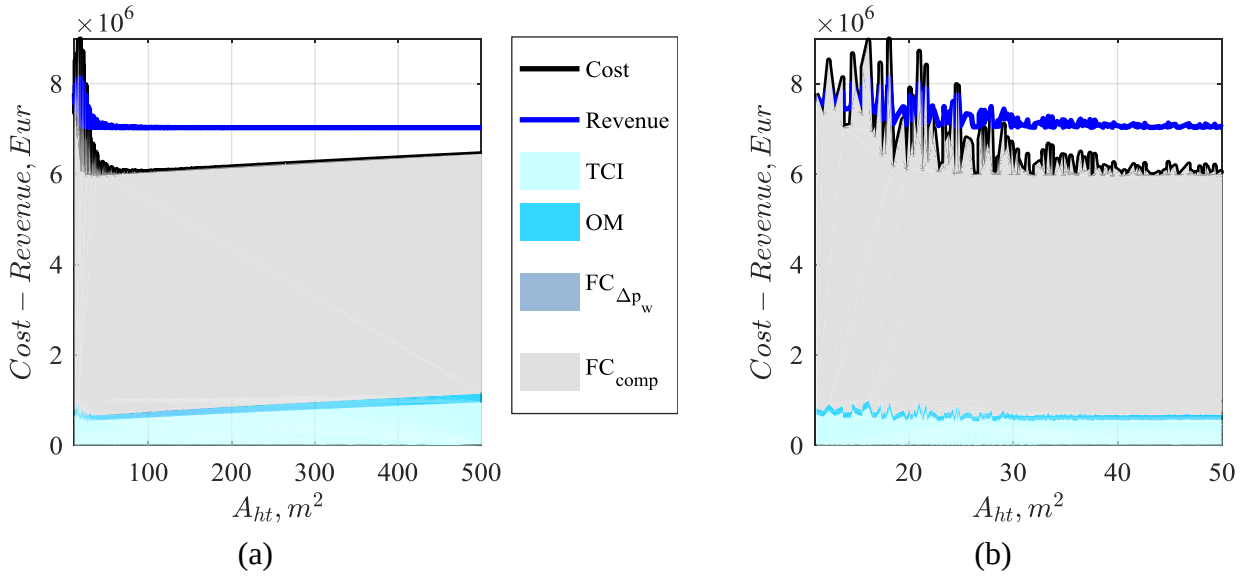

Fig. 9. Breakdown of the NPV terms as function of A_{ht}, with separation between annualised cost and revenue. The different coloured areas indicate the different contributions to the cost term. Results are reported for the whole solution space (a) and close-up with area up to 50 m^2 (b)

First of all, it was shown that the running costs for the water pressure drop are several orders of magnitudes lower than the other contributions, so that they are not visible in the cost breakdown. Moreover, it was observed that the most relevant contribution to the cost was given by the running cost of the compressor, indicated by the grey area. As expected, the running cost was not constant over the different PHE heat transfer areas. In fact, when the heat transfer area was minimized, the mixture experienced higher pressure losses, hence requiring a higher compressor work, and strongly impacting the economy of the heat pump. The cost line (in black) overcame the revenue line (in blue) for some configurations with small area, which is clearly visible in the close-up in Fig. 9 (b).

Lastly, it was shown that TCI and OMC constitute the other relevant sources of cost, and that the TCI tended to increase with increasing areas. However, the TCI oscillated in the lower range of PHE area, and despite the minimization of PHE investment costs, the compressor sizing influenced the results,

as shown in Fig. 10 (a), where the different investment costs are reported as function of the PHE heat transfer area. In fact, this region corresponded to the lowest contribution of the PHE to the TCI, yet the compressor sizing considering pressure drops could be consistently higher for those configurations with unfavourable pressure losses. Therefore, the figure shows the trade-off between compressor and evaporator contributions to the investment cost. The condenser curve was constant as the design was fixed based on the previous study design criterion [3].

Fig. 10 (b) summarizes the impact of the heat transfer area, i.e. the different design of the PHE, on the NPV, and colours indicating the liquid phase Reynolds number, chosen as flow design parameter. It was confirmed that the optimal region of Case I corresponded to values of Reynolds around 1,000 to 1,500.

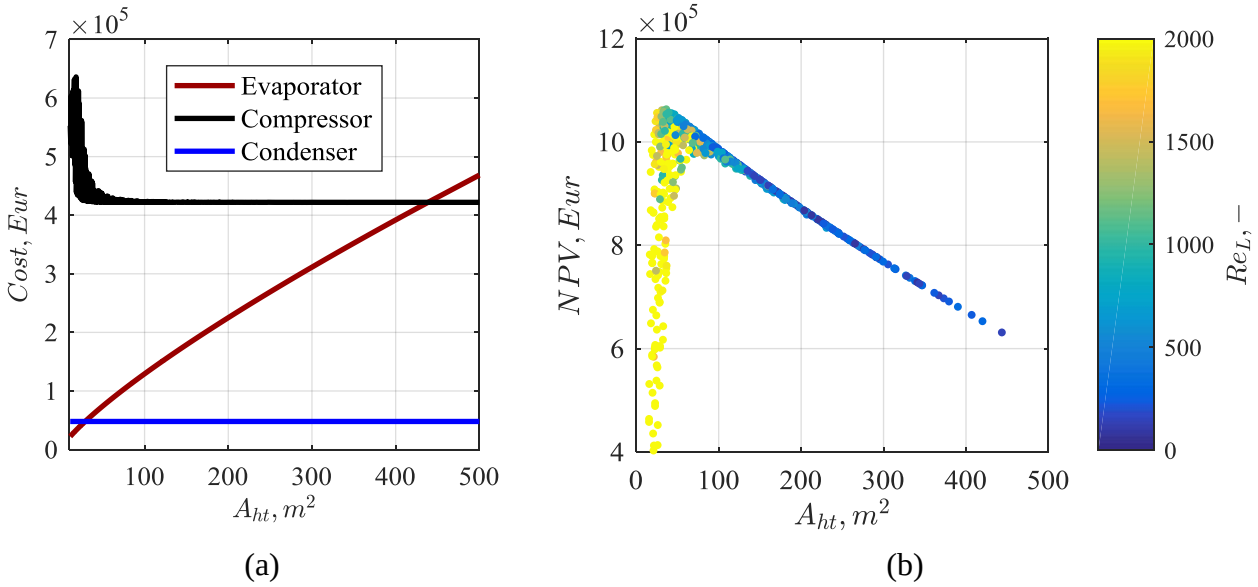

Fig. 10. (a) Investment costs of evaporator, compressor and condenser as function of the evaporator heat transfer area (b) NPV as function of the heat transfer area, with colours indicating the liquid Reynolds number at evaporator inlet

3.6. Design point

To conclude the results section, the trade-off between the PHE heat transfer area and the pressure losses is presented for the best solution of the four cases, corresponding to the heat exchanger configurations maximizing the NPV of the heat pump. The results are reported in Table 3, where heat transfer area, total capital investment cost, pressure drops of mixture and water and liquid Reynolds number at the evaporator inlet are indicated. It is shown that Case I and Case IV corresponded to the mixtures in which the optimal design required a lower pressure drop of the working fluids, thus a higher heat transfer area of the heat exchanger. Similarly to what was obtained in the preliminary analysis [3], Case I and II correspond to higher NPVs, due to the higher investment costs for Case III and Case IV, even for the best design solutions.

Table 3. Best solutions in terms of NPV for the four considered cases

	Unit	Case I	Case II	Case III	Case IV
COP	–	3.06	3.05	3.01	3.05
NPV	10^3 eur	1,060	1,135	617	641
A_{ht}	m^2	37.40	21.70	23.10	40.30
TCI	10^3 eur	548	461	852	885
Δp_{mix}	Pa	5,257	16,168	26,937	2,064
Δp_w	Pa	2,234	14,613	7,347	796
$Re_{L_{inlet}}$	–	1,128	2,260	1,434	523

It has to be mentioned that the parametric analysis considered 900 combinations of design parameters. Several optimal solutions, with very small differences of NPV, were found with different combinations of design parameters. Therefore, the comparison between the two most optimal solutions of Case I are presented in order to highlight the differences, and to show the obtained PHE design specifications; results are reported in Table 4. It is shown that the NPV of the second best solution differs of 0.025% compared to the best case, i.e. both points can be considered as optimal for the evaporator design.

The full specification set (plate size and plate corrugation) of the two solutions shows that in the first case, a design with wider plates and smaller number of channels is preferred, whilst in the second case higher length-to-width ratio is achieved, with a lower width and higher number of channels. This confirms the results shown in the previous section, which highlighted how optimal configurations could be achieved by different combinations of plate size and numbers. On the other hand, it is shown that similar corrugation characteristics are employed in both cases, lying in the optimal range before identified. Therefore, the results seem to be strongly influenced mostly by the plate corrugation.

Table 4. PHE specifications for Case I best solutions

	Unit	Case I – Best solution	Case I – Second best solution
COP	–	3.06	3.06
NPV	10^3 eur	1,060	1,059
General PHE design characteristics:			
A_{ht}	m^2	37.4	32.1
Δp_{mix}	Pa	5,256	8,139
Δp_w	Pa	2,234	46,132
$Re_{L_{inlet}}$	–	1,128	1,409
Plate size:			
W	m	0.5	0.1
N_{ch}	–	10	40
L_{th}	m	0.44	0.45
L_{th}/W	–	0.88	4.5
Plate corrugation:			
b	m	0.008	0.008
Λ	m	0.002	0.002
β	°	45	45
D_h	m	0.002	0.002
X	–	12.6	12.6

4. Discussion

The analysis presented in this work shows the influence of the design of a PHE evaporator on the NPV of a heat pump, using four different zeotropic mixtures as working fluid. The shown trends are similar for the four considered cases, yet the extension to more general applications with the use of zeotropic mixtures would require a more comprehensive study. In fact, it is very relevant to clarify the range of validity of the obtained results, tested considering only four possible working fluids used in a case study. The PHE optimal configurations, reported in Table 3, show the impact of using different working fluid mixtures on defining an optimal Reynolds number, thus the extension of the obtained recommendations to other type of mixtures requires validation.

Furthermore, the definition of an optimal Reynolds number might be dependent on cycle constraints, which make these design recommendations useful only when considering evaporators with similar conditions of the working fluid at the inlet. A similar consideration can be done on the water pressure

drop influence on the NPV, which is shown as negligible compared to the other contributions. Changing the temperature and pressure levels, and heat source medium, can influence the results.

Additionally, it was shown that the results were not dependent on the choice of the plate size, thus length-to-width ratio and number of channels could be adjusted according to the designer decision without affecting the possibility of reaching an economically optimal solution. However, the PHE numerical model does not take into account the mass flow distribution inside the channels, as well as the vapour and liquid distribution, which might lead to completely different results for some of the configurations. Therefore, an extension is required to describe the impact of the number of channels and distribution effect on the design.

A further point is given by the methodology followed in the work, which is based on a parametric study of the PHE, hence limiting the search space of the optimal solution. Implementing a full optimization procedure could be considered as a future extension.

Lastly, the results are dependent on the economic assumptions of interest rate, cost of electricity, as well as operational time of the plant. By changing these inputs, the impact on the NPV might be affected, hence requiring a further sensitivity study.

5. Conclusions

The parametric analysis conducted on the main parameters of the PHE shows that it is possible to derive design guidelines that can be potentially used in applications where PHEs are used as evaporators in heat pumps using zeotropic mixtures. The method applied is based on a combined evaluation of cycle performances and calculation of PHE required heat transfer area and pressure losses. The result shows that there are combinations of design parameters, which are optimal for the NPV of the heat pump, for all the considered cases. It is shown that the optimal design regions does not coincide with the design point adopted in a previous study, based on a practical limitations of the maximum inlet velocity, without accounting for the pressure losses of the PHE in the thermodynamics and economic calculations.

The results highlight design guidelines for the optimal PHE corrugation geometry, i.e. values of corrugation height around 8mm combined with low corrugation pitches around 2mm creates low hydraulic diameter, which are able to create a high degree of turbulence without increasing excessively the total pressure losses. From the results, it is obtained that the plate size, namely plate-to-width ration and number of channels, do not have a clear correlation with the NPV of the cycle, i.e. optimal solutions can be found by adopting different plate sizes, and adjusting number of channels and corrugation geometry accordingly. An optimal range is found for the liquid Reynolds number at the evaporator inlet, and it is recommended to keep the value within the range 500-2,000. The interval found is broad since the results are dependent on the working fluid considered.

Moreover, an in-depth cost analysis has shown the trade-off between heat transfer area and pressure losses, by considering all the contributions to the NPV calculations. It is obtained that it is not convenient to minimize the heat exchanger area without considering the mixture pressure drops, since the investment and running cost of the compressor are negatively impacted. On the other hand, the pressure losses of the heat source side, i.e. water, do not influence the results of the economic calculations.

Acknowledgments

This research project is financially funded by the Danish Council for Strategic Research in Sustainable Energy and Environment, under the project title: “THERMCYC – Advanced thermodynamic cycles utilising low temperature heat sources". The support is gratefully acknowledged.

Nomenclature

A	Area, m^2	NPV	Net Present Value, €
b	Corrugation height, mm	p	Pressure, Pa
c_{el}	Price of electricity, €/kWh	PEC	Purchased equipment cost, €
COP	Coefficient of Performance	Q	Vapour quality
CRF	Capital recovery factor	R	Thermal resistance, $(m^2K)/W$
D	Diameter, mm	Re	Reynolds number
f	Friction factor	t	Plate thickness, mm
FC	Fuel cost, €/yr	TCI	Total Capital Investment, €
G	Mass velocity, $kg/(m^2s)$	U	Overall heat transfer coefficient, $W/(m^2K)$
h	Heat transfer coefficient, $W/(m^2K)$	$\dot{V}$	Volumetric flow rate, m^3/h
L_{th}	Plate length, m	W	Plate width, m
$\dot{m}$	Mass flow, kg/s	X	Corrugation characteristic
N_{ch}	Number of channels		

Greek symbols

β	Chevron angle, °	ρ	Density, kg/m^3
Φ	Enlargement factor	μ	Viscosity, Pa s
Λ	Corrugation pitch, mm	τ	Time, h
η	Efficiency		

Abbreviations

CV	Control Volume	PHE	Plate Heat Exchanger
ORC	Organic Rankine Cycle		

Subscripts

acc	acceleration	*L*	liquid
core	core	*m*	median
e	equivalent	*mix*	mixture
fr	friction	*ng*	natural gas
h	hydraulic	*o*	outlet
hp	heat pump	*p*	port
ht	heat transfer	*w*	water
i	inlet		

References

[1] F. Bühler, T.-V. Nguyen, and B. Elmegaard, "Energy and exergy analyses of the Danish industry sector" *Applied Energy*, vol. 184, pp. 1447–1459, Feb. 2016.

[2] IEA Heat Pump Centre - Annex 35, "Application of Industrial Heat Pumps - Final report" Borås, Sweden, 2014.

[3] B. Zühlsdorf, F. Bühler, R. Mancini, S. Cignitti, and B. Elmegaard, "High Temperature Heat Pump Integration using Zeotropic Working Fluids for Spray Drying Facilities" in *Proceedings of the 12th IEA Heat pump conference, Rotterdam*, 2017.

[4] R. Radermacher and Y. Hwang, *Vapor Compression Heat Pumps with Refrigerant Mixtures*. CRC Press 2005, 2005.

[5] M. M. Abu-Khader, "Plate heat exchangers: Recent advances" *Renewable & Sustainable Energy Reviews*, vol. 16, no. 4, pp. 1883–1891, 2012.

[6] J. a. W. Gut and J. M. Pinto, "Optimal configuration design for plate heat exchangers" *International Journal of Heat and Mass Transfer*, vol. 47, no. 22, pp. 4833–4848, 2004.

[7] S. Karellas, A. Schuster, and A.-D. Leontaritis, "Influence of supercritical ORC parameters on plate heat exchanger design" *Applied Thermal Engineering*, vol. 33–34, pp. 70–76, 2012.

[8] J. Wang, M. Wang, M. Li, J. Xia, and Y. Dai, "Multi-objective optimization design of condenser in an organic Rankine cycle for low grade waste heat recovery using evolutionary algorithm" *International Commununications of Heat and Mass Transfer*, vol. 45, pp. 47–54, 2013.

[9] N. Rohmah, G. Pikra, A. J. Purwanto, and R. I. Pramana, "The Effect of Plate Spacing in Plate Heat Exchanger Design as a Condenser in Organic Rankine cycle for Low Temperature Heat Source" *Energy Procedia*, vol. 68, pp. 87–96, 2015.

[10] D. Walraven, B. Laenen, and W. D'Haeseleer, "Comparison of shell-and-tube with plate heat exchangers for the use in low-temperature organic Rankine cycles" *Energy Conversion and Management*, vol. 87, pp. 227–237, 2014.

[11] VDI-Gesellschaft, *VDI Heat Atlas*, vol. 1. 2015.

[12] Mathworks, "Matlab R2016b." [Online]. Available: https://www.mathworks.com/products/new_products/latest_features.html, accessed: 07th February 2017.

[13] National Institute of Standard and Technology, "Reference Fluid Thermodynamic and Transport Properties Database version 9.1" [Online]. Available: https://www.nist.gov/srd/refprop, accessed: 07th February 2017.

[14] R. K. Shah and D. P. Sekulic, *Fundamentals of Heat Exchanger Design*. 2002.

[15] J. K. Jensen, M. R. Kaernl, T. S. Ommen, W. Brix, L. Reinholdt, and B. Elmeegard, "Effect of liquid/vapour maldistribution on the performance of plate heat exchanger evaporators" in *Proceedings of the 24th IIR International Congress of Refrigeration*, 2015.

[16] H. Martin, "A theoretical approach to predict the performance of chevron-type plate heat exchangers" *Chemical Engineering and Processing: Process Intensification*, vol. 35, no. 4, pp. 301–310, 1996.

[17] D. S. Jung, M. McLinden, R. Radermacher, and D. Didion, "A study of flow boiling heat transfer with refrigerant mixtures", *International Journal of Heat and Mass Transfer*, vol. 32, no. 9, pp. 1751–1764, 1989.

[18] D. S. Jung and R. Radermacher, "Prediction of pressure drop during horizontal annular flow boiling of pure and mixed refrigerants," *International Journal of Heat and Mass Transfer*, vol. 32, no. 12, pp. 2435–2446, 1989.

[19] T. Ommen, J. K. Jensen, W. B. Markussen, L. Reinholdt, and B. Elmegaard, "Technical and economic working domains of industrial heat pumps: Part 1 - Single stage vapour compression heat pumps," *International Journal of Refrigeration*, vol. 55, pp. 168–182, 2015.

[20] A. Bejan, G. Tsatsaronis, and M. Moran, *Thermal design and optimization*. John Wiley and Sons, Inc., 1996.

[21] SWEP International AB, "SWEP." [Online]. Available: http://www.swep.net/, accessed: 07th February 2017.

[22] "Alfa Laval," 2015. [Online]. Available: http://www.alfalaval.com/, accessed: 07th February 2017.